Supporting Information for

Insights into the kinetics of supramolecular comonomer incorporation in water

*René P. M. Lafleur, Sandra M. C. Schoenmakers, Pranav Madhikar, Davide Bochicchio, Björn Baumeier, Anja R. A. Palmans, Giovanni M. Pavan, and E. W. Meijer**

Contents

Instrumentation and materials. HDX-MS measurements were carried out using a Xevo G2 QTof mass spectrometer (Waters) with a capillary voltage of 2.7 kV, a sampling cone voltage of 80 V and an extraction cone voltage of 4.0 V. The source temperature was set at 100 °C, the desolvation temperature at 400 °C, the cone gas flow at 10 L/h and the desolvation gas flow at 500 L/h. The sample solutions subjected to HDX were introduced into the mass spectrometer using a Harvard syringe pump (11 Plus, Harvard Apparatus) at a flow rate of 50 µL/min, and the signal was accumulated during 60 seconds.

Stopped-flow UV-Vis measurements were performed with a BioLogic stopped-flow setup consisting of a MOS-500 spectrometer with Xe/Hg light source, an ALX 250 Arc Lamp Power Supply, SAS PMT-450 photomultiplier tube, an SFM-400/S stopped-flow module with an MPS-60 microprocessor unit and a Julabo F-12 temperature control system. BioKine 32 software was used to operate the stopped-flow setup. All measurements were performed at a wavelength of 229 nm, with a bandwidth of 1 nm and using a sampling time of 1 sec. The high voltage (HV) applied on the photomultiplier tube was set at a constant 340 V. Samples were mixed in a 1:1 ratio at a flow rate of 14 mL/s. All measurements were performed using a BioLogic TC-100/10C cuvet with a path length of 1 cm, and at a temperature of 20 °C.

UV-Vis absorbance spectra were recorded on a Jasco V-650 UV-Vis spectrometer equipped with a Jasco ETCT-762 temperature controller. Measurements were performed in a Quartz cuvet with a path length of 1 cm at 20 °C, and were corrected using MQ-water as a baseline. All measurements were performed with a bandwidth of 1.0 nm, a scan speed of 100 nm/min and a data interval of 0.1 nm, spanning the UV-Vis range of 350 nm to 190 nm. The turbidity measurements were performed with a bandwidth of 1.0 nm and were recorded at 340 nm by sampling every 0.5 °C. A heating-cooling program with a start temperature of 20 °C, a temperature ramp of 0.2 °C/min and a maximum temperature of 90 °C was used. Some hysteresis was observed between the heating and cooling curves. Since the latter displayed the clearest transitions, the cooling curves were used to create Figure 2 in the main text.

Infrared spectra were recorded on a Perkin Elmer Spectrum Two FT-IR spectrometer, equipped with a Perkin Elmer Universal ATR Sampler Accessory. Solution FT-IR measurements were performed using a CaF_2 Liquid Cell with an optical path length of 0.05 mm. For the solution samples, first a background of the appropriate solvent was measured. All spectra were measured at room temperature from 700 cm^{-1} to 4000 cm^{-1}. The solid state samples were averaged over 16 scans and the solution samples were averaged over 128 scans.

Samples for CryoTEM imaging were vitrified using a computer controlled vitrification robot (FEI Vitrobot^{TM} Mark III, FEI Company). Lacey films (LC200-CU, Electron Microscopy Sciences) were surface plasma treated with a Cressington 208 carbon coater. Vitrified films were transferred into the vacuum of a CryoTITAN equipped with a field emission gun that was operated at 300 kV, a post-column Gatan energy filter, and a 2048 x 2048 Gatan CCD camera.

The synthesis of the BTAs used in this manuscript was reported previously.[S1] The water used to prepare the BTA samples was purified on an EMD Millipore Milli-Q Integral Water Purification System, and subsequently filtered using a 0.2 µm syringe filter (Supor membrane, PALL Corporation).

BTA sample preparation. The solid C_{12}BTA was weighed out and added to a glass vial. Filtered MQ-water was added to obtain a concentration of 50 µM. The mixture was stirred, with a magnetic stirring bar, at 80 °C for 15 minutes. The hot and hazy mixture was vortexed for 15 seconds and was subsequently left to equilibrate at room temperature overnight. Since C_{10}BTA is an oily substance, it was transferred from the weighing boat to the glass vial with $CHCl_3$. The $CHCl_3$ was evaporated by blowing a constant stream of N_2 (g) 1 cm above the solvent level, before filtered MQ-water was added to obtain a concentration of 50 µM. The same heating and vortexing protocol as used for C_{12}BTA was followed. C_{13}BTA samples were prepared by adding the solid material to a glass vial. Approximately 300 µL $CHCl_3$ was added and the sample was vortexed for 15 seconds to dissolve the BTA. The $CHCl_3$ was evaporated with a stream of N_2 (g) approximately 1 cm above the solvent level. Then, filtered MQ-water was added to obtain a concentration of 50-100 µM. The sample was stirred, with a magnetic stirring bar, at 80 °C for 15 minutes. Subsequently, the hot and hazy mixture was vortexed for 15 seconds and was left to equilibrate at room temperature overnight. The next day, the C_{13}BTA sample was filtered with a 0.2 µm syringe filter (Supor membrane, PALL Corporation) to remove precipitates. By blowing a constant stream of N_2 (g) 1 cm above the solvent level, while stirring, water was evaporated from the sample to increase the concentration to 50 µM. The concentration was determined with UV-spectroscopy, using calibration curves based on the absorbance of C_{12}BTA at 250 nm. All samples were left to equilibrate overnight before the copolymerization experiments. UV-spectra recorded of copolymers (Figure S4) were recorded 24 h after mixing. The mixtures containing two BTAs that were used for the turbidity experiments were equilibrated 24 h before use. The mixtures used for CryoTEM imaging (Figure S3) were also prepared 24 h in advance by combining equimolar solutions of C_{10}BTA with C_{12}BTA or C_{13}BTA at RT and in a 1:1 ratio. However, in this case the concentration of the individual BTA solutions (prepared one day before the mixing step) was 600 µM.

HDX-MS of copolymerization. To study the incorporation of C_{10}BTA into a supramolecular polymer with HDX-MS, 50 µM samples of the pre-assembled C_{10}BTA were added to 50 µM samples of a supramolecular polymer (at t = 0 min), and a timer was started. The samples were vortexed for 3 seconds to mix the samples. 20 µL aliquots of this sample in H_2O were periodically taken and were diluted 10 times into D_2O (including 0.5 mM sodium acetate to facilitate the detection), by adding 180 µL D_2O using a micropipette. All samples were stored at room temperature during the course of the HDX experiments (~ 20°C). Within 30 seconds the diluted samples were transferred to the syringe. Samples were injected with a syringe pump and the signal was left to equilibrate for one minute before starting the measurement. The measurements were started exactly 90 seconds after the dilution according to the timer, and they were accumulated over one minute at a flow rate of 50 µL/min to account for instabilities in the signal. Before the measurements, the system was calibrated.

Calculating the percentage of BTA3D and BTA6D. Because 20 µL of the BTA sample solutions in water were diluted into 180 µL D_2O, 10 vol% of H_2O was present in the diluted samples. This results in monomers with incomplete HDX, hence BTA-1D, BTA-2D, BTA-4D and BTA-5D will be detected. The statistical ratio BTA-1D : BTA-2D : BTA-3D is

$3.7x10^{-3}$: $8.3x10^{-2}$: 1 and the statistical ratio BTA-4D : BTA-5D : BTA-6D is $1.9x10^{-1}$: $6.7x10^{-1}$: 1. Therefore, we took the presence of BTA-2D, BTA-4D and BTA-5D into account when calculating the percentage of BTA-3D and BTA-6D. Moreover, all intensities were corrected for the isotope overlap of BTA-3D. The isotope patterns were calculated with Bruker Compass IsotopePattern. For C_{10}BTA-3D and C_{10}BTA-6D, this resulted in the following formula's:

$$C_{10}\text{BTA-3D\%} = \frac{I_{626.42}}{I_{625.92} + I_{626.42} + (I_{626.92} - 0.71I_{626.42}) + (I_{627.42} - 0.29I_{626.42}) + (I_{627.93} - 0.08I_{626.42})} \times 100\% ,$$

$$C_{10}\text{BTA-6D\%} = \frac{I_{627.93} - 0.08I_{626.42}}{I_{625.92} + I_{626.42} + (I_{626.92} - 0.71I_{626.42}) + (I_{627.42} - 0.29I_{626.42}) + (I_{627.93} - 0.08I_{626.42})} \times 100\% ,$$

with $I_{626.42}$ the intensity corresponding to C_{10}BTA-3D and $I_{625.92}$ the intensity corresponding to C_{10}BTA-2D. ($I_{626.92}$-0.71$I_{626.42}$) is the intensity corresponding to C_{10}BTA-4D, ($I_{627.42}$-0.29$I_{626.42}$) is the intensity corresponding to C_{10}BTA-5D, and ($I_{627.93}$-0.08$I_{626.42}$) is the intensity corresponding to C_{10}BTA-6D, with 0.71, 0.29 and 0.08 following from the calculated isotope patterns. To calculate the percentage of BTA3D of the other BTAs, similar formula's were applied:

$$C_{12}\text{BTA-3D\%} = \frac{I_{668.46}}{I_{667.96} + I_{668.46} + (I_{668.97} - 0.78I_{668.46}) + (I_{669.47} - 0.34I_{668.46}) + (I_{669.97} - 0.10I_{668.46})} \times 100\%$$

$$C_{13}\text{BTA-3D\%} = \frac{I_{689.47}}{I_{688.97} + I_{689.47} + (I_{689.97} - 0.81I_{689.47}) + (I_{690.47} - 0.36I_{689.47}) + (I_{690.98} - 0.12I_{689.47})} \times 100\%$$

Fitting the percentage of C_{10}BTA-3D. The percentage of C_{10}BTA-3D was averaged over three measurements and was plotted as a function of time using Origin 2015. These kinetic traces were fitted with functions available in Origin 2015; the percentage of C_{10}BTA-3D in the mixtures was fitted with the ExpGro2 function, y = A1*exp(t/t1) + A2*exp(t/t2) + y0 and with the ExpGro1 function, y = A1*exp(t/t1) + y0. A1, t1, A2, t2 and y0 are the parameters being varied during the fitting and t is the independent variable (time in minutes). A statistical F-test was subsequently used to determine whether the data was best described with a mono-exponential fit or of a bi-exponential fit, with the null-hypothesis that the mono-exponential fit describes the data best. The F-statistic was calculated with $F=((SS_1-SS_2)/(df_1-df_2))/(SS_2/df_2)$, with df_1 the degree of freedom of the mono-exponential fit, df_2 the degree of freedom of the bi-exponential fit, SS_1 the residual sum of squares of the mono-exponential fit and SS_2 the residual sum of squares of the bi-exponential fit. All values could be obtained from Origin 2015. The corresponding p-value for $\alpha = 0.05$ was obtained from the software package Rcmdr. The null-hypothesis was rejected when the p-value was lower than α. We concluded that a bi-exponential growth function is required to fit the data for 1 C_{10}BTA:1 C_{12}BTA ($\alpha = 0.05$, $p = 0.0002$), while the statistical f-test indicated that a mono-exponential growth function is sufficient to fit the data for 1 C_{10}BTA:1 C_{13}BTA ($\alpha = 0.05$ and $p = 0.361$).

The data for 1 C_{10}BTA:1 C_{12}BTA was described with C_{10}BTA-3D = -10.58*exp(t/(-2.69)) – 4.22*exp(t/(-29.41)) + 14.60 (R^2_{adj} = 0.9972). The data for 1 C_{10}BTA:1 C_{13}BTA was best described with C_{10}BTA-3D = -12.26*exp(t/(-18.28)) + 12.67 (R^2_{adj} = 0.9919).

The t_{50} was calculated by fitting the percentage of C_{10}BTA-3D of the three individual measurements to a bi-exponential or mono-exponential growth function. From the resulting fitting equations the time required to reach 50% of the maximum percentage of BTA-C_{10}-3D was calculated. The average t_{50}'s and standard deviations are mentioned in the main text.

Stopped-flow UV-measurements and fitting. The measurements were analyzed with Origin 2015 by normalizing the average UV absorbance of three measurements. To calculate the t_{50}'s, the UV-absorbance of the three individual measurements was fitted with Origin's mono-exponential growth (ExpGro1, see above) function (R^2_{adj} > 0.86 for all fits) starting from the minima. From the fits we calculated the time required to reach 50% of the maximum UV-absorbance. The average t_{50}'s and standard deviations are mentioned in the main text.

CryoTEM imaging. Vitrified films containing the mixtures were prepared in the 'Vitrobot' that was operated at 22°C, and at a relative humidity of 100%. In the preparation chamber of the 'Vitrobot', a 3µl sample was applied on a Lacey grid which was surface plasma treated for 40 s at 5 mA just prior to use. Excess sample was removed by blotting using two filter papers for 3 s at –3 mm, and the thin film thus formed was plunged (acceleration about 3 g) into liquid ethane just above its freezing point. Virtrified films were observed in the CryoTITAN microscope at temperatures below -170 °C. Micrographs were taken at low dose conditions, starting at a magnification of 6500 with a defocus setting of 40 µm, and at a magnification of 24000 with a defocus setting of 10 µm.

Probing hydrogen bonds by infrared spectroscopy. Samples for FT-IR were prepared at a concentration of 50 mg/mL for C_{10}BTA and C_{12}BTA, and at a concentration of 20 mg/mL for C_{13}BTA (without filtering). BTA material was weighed and added to a clean vial. All samples were dried overnight with approximately 5 grams of P_2O_5 in a separate beaker in a vacuum oven at 40 °C. Samples in MeOD were prepared by adding solvent to the vials to obtain the desired concentration and the samples were left to equilibrate overnight. Aliquots of these samples were dried with a stream of N_2 (g) to yield the deuterated solid BTA. Samples in D_2O were prepared by stirring the samples at 80 °C for 15 minutes after adding the solvent. The hot and hazy samples were subsequently vortexed for 15 seconds and were left to equilibrate at room temperature overnight. All equilibrated samples in D_2O were slightly hazy and viscous. The C_{13}BTA sample was subjected to repetitive rounds of vortexing and sonication (30 seconds each) before it was heated to assemble the molecules. The samples in MeOD were injected into the FT-IR Cell with a syringe. Samples in D_2O were injected by pipetting small aliquots of the sample into the FT-IR Cell.

Previously we used FT-IR to confirm that intermolecular hydrogen bonds are formed between the monomers of C_{12}BTA when assembled in water.[S1] The FT-IR spectrum of C_{12}BTA in the solid state displays three vibrations characteristic for intermolecular hydrogen bonding: an N-H stretch (3400-3300 cm^{-1}), an amide I (C=O stretch, 1700-1600 cm^{-1}) and an amide II vibration (N-H bend, 1600-1500 cm^{-1}) (Figure S1A). Especially the amide I vibration is of

interest, because the other vibrations interfere with vibrations from the solvent. Since O-H vibrations of water molecules overlap with the amide vibrations of the BTAs, we used D_2O as a solvent. To correctly assign the peaks, a solid C_{12}BTA sample with all labile hydrogen atoms exchanged for deuterium was measured first (Figure S1A). For unknown reasons, the amide I vibration is splitted into vibrations at 1634 and 1620 cm^{-1} when the amides are deuterated. In MeOD the BTAs are molecularly dissolved and no hydrogen bonds are present, resulting in a single amide I vibration located at 1648 cm^{-1}. The peaks between 2600 and 2000 cm^{-1} are due to scattering of some large particles in the sample. When assembled in D_2O, the amide I vibration of C_{12}BTA at 1620 cm^{-1} disappeared and only a vibration at 1635 cm^{-1} is observed. This is a clear shift compared to the amide I vibration in MeOD, in which no hydrogen bonds were present. Hence, this confirms our previous results and we used the same procedure to study the formation of intermolecular hydrogen bonds in assemblies of C_{10}BTA and C_{13}BTA. Since the amide I region of the spectra in MeOD and D_2O are of most interest, only this region is displayed (Figure S1B). The amide vibrations for C_{13}BTA are lower in intensity due to the lower sample concentration. In MeOD all BTAs show an amide I vibration at 1648 cm^{-1}, indicative for the absence of hydrogen bonds. In D_2O, C_{13}BTA has an amide I vibration at 1635 cm^{-1}, similar to C_{12}BTA. This indicates that these assemblies are stabilized by the presence of intermolecular hydrogen bonds. For C_{10}BTA, the assemblies in D_2O result in a broad peak centered around 1641 cm^{-1}. This indicates that, even at the much higher BTA concentration (50 mg/mL) as compared to the turbidity measurements (0.06 mg/mL for C_{10}BTA (50 µM)), the hydrogen bonds are less pronounced in C_{10}BTA assemblies as compared to the other assemblies.

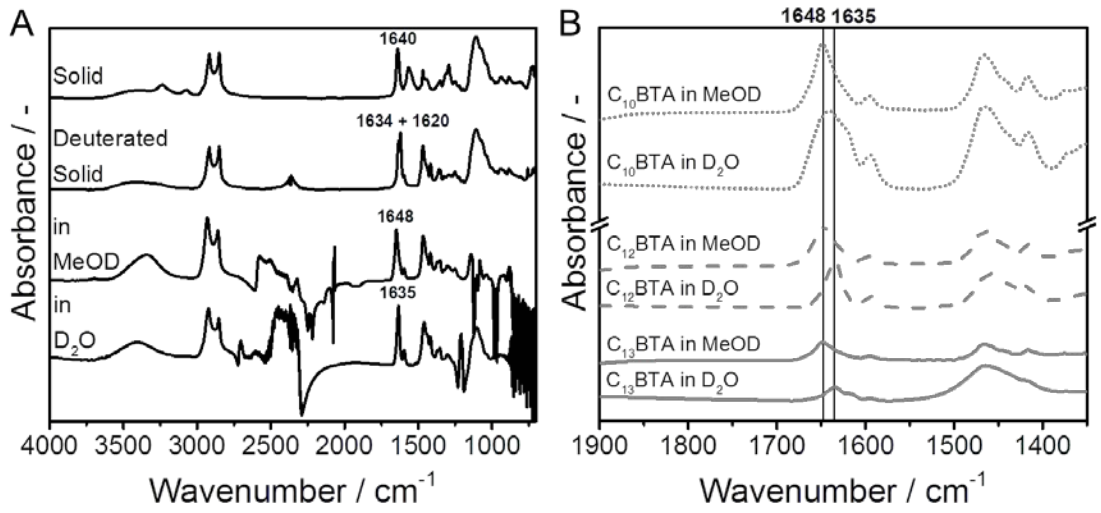

Figure S1. A) FT-IR spectra of the C_{12}BTA, from top to bottom: as a solid, a deuterated solid, in MeOD (50 mg/mL) and in D_2O (50 mg/mL), with the wavenumbers of the amide I vibrations. B) Zoom of the amide I vibration region of the FT-IR spectra recorded for all BTAs in MeOD and D_2O. The measurements were performed with a path length of 0.05 mm and at RT.

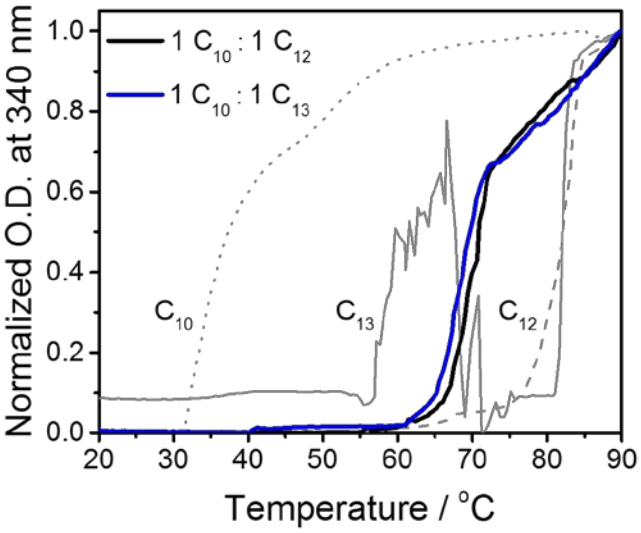

Figure S2. Heating curves of the turbidity measurements that were recorded before the cooling curves as displayed in Figure 2 of the manuscript, showing the normalized UV-absorption at 340 nm as a function of temperature for the single component aggregates: C_{10}BTA (grey, dot), C_{12}BTA (grey, dash) and C_{13}BTA (grey, solid), and the dual component polymers with C_{10}BTA and C_{12}BTA (black), and C_{10}BTA and C_{13}BTA (blue). The heating rate was 0.2°C/min, the concentration 50 µM, the path length of the quartz cuvette used was 1 cm, and the measurements were performed without stirring.

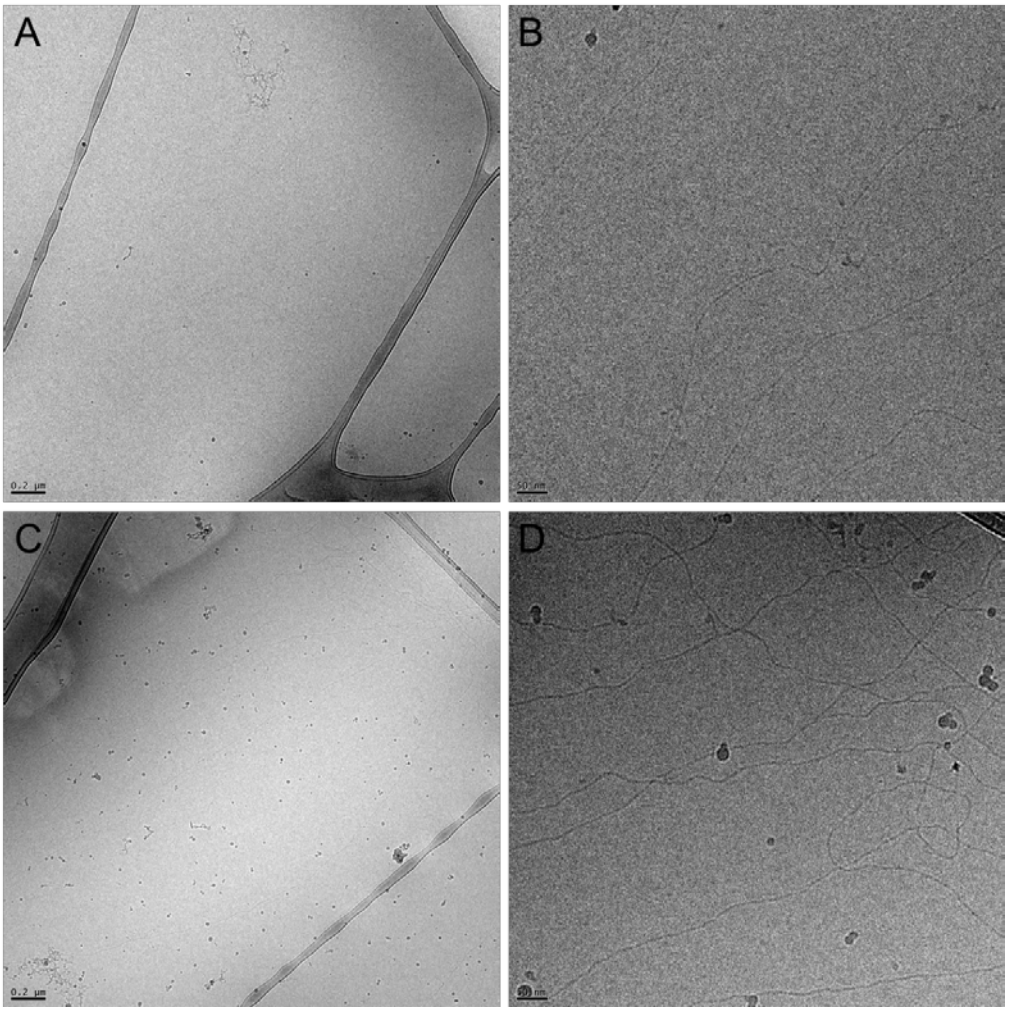

Figure S3. Cryo-TEM images from samples that were vitrified 24 hours after mixing 600 µM C_{10}BTA with 600 µM C_{12}BTA (A and B), and 600 µM C_{10}BTA with 600 µM C_{13}BTA in MQ-water (C and D), in a 1:1 (v:v) ratio. A) CryoTEM image (scale bar is 200 nm) at a magnification of 6500 and 40 µm below focus, with B) the corresponding high magnification image (scale bar is 50 nm) at 24000 and 10 µm below focus, revealing the presence of supramolecular polymers with a high aspect ratio. C) CryoTEM image (scale bar is 200 nm) at a magnification of 6500 and 40 µm below focus, with D) the corresponding high magnification image (scale bar is 50 nm) at 24000 and 10 µm below focus, revealing the presence of supramolecular polymers with a high aspect ratio. All images feature some black (high-contrast) sphere-like objects that are crystalline ice particles, and in the top left corner of C) some hexagonal ice contamination is present.[S2]

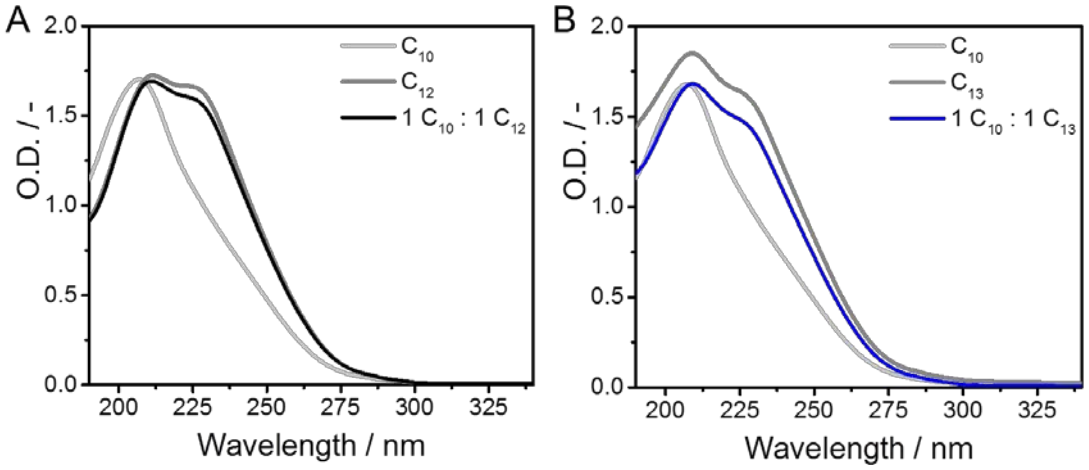

Figure S4. UV-absorption spectra recorded 24 hours after the mixing of C_{10}BTA in a 1:1 ratio with A) C_{12}BTA (black line) and B) C_{13}BTA (blue line). The UV-spectrum of C_{10}BTA is shown in light grey and the UV spectra of C_{12}BTA and C_{13}BTA are displayed in dark grey. The UV-absorption spectra of the mixtures at a 1:1 molar ratio have a similar shape as compared to the spectra of the host polymers. The samples were equilibrated and measured at 20°C, at a concentration of 50 µM in water with a 1 cm path length cuvette.

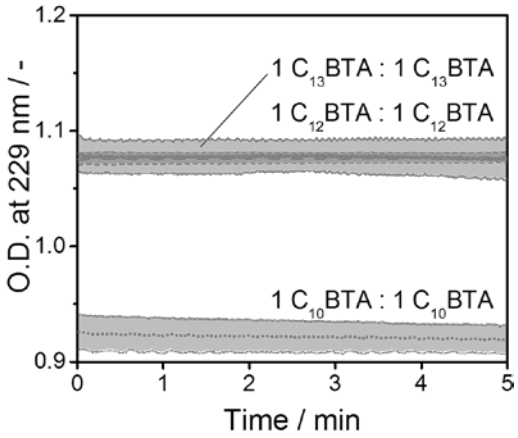

Figure S5. UV-absorbance at 229 nm as a function of time after the 1:1 mixing of equally concentrated BTA solutions containing the same BTA: C_{10}BTA (grey, dot), C_{12}BTA (grey, dash) and C_{13}BTA (grey, solid), at a concentration of 50 µM (path length = 1 cm, T = 20°C). The lines are an average of four measurements and the surrounding areas represent one standard deviation of uncertainty.

Design of the HDX-MS experiment. In this example, the C_{10}BTA was mixed with polymers formed from the C_{12}BTA. The concentration of the equimolar solutions was 50 µM in H_2O and for the HDX pulse an aliquot of the mixture was diluted 10-fold in D_2O. Because of the ESI settings that were used (see above), full depolymerization occurs during mass spectrometry and only monomers can be observed. This allowed us to analyze the extent of HDX by assessing the molecular weights of both monomers that are present in the mixture.

One minute after mixing C_{10}BTA and C_{12}BTA in H_2O, we diluted an aliquot of the mixture into D_2O and performed ESI-MS. The mass spectrum was observed to display almost exclusively peaks belonging to fully deuterated C_{10}BTA-6D (Figure S6A). The base peak at m/z 627.9 corresponds to the double sodium adduct of C_{10}BTA-6D, that was observed to be the most prominent ion. The peaks to the right of the base peak at 627.9 originate from the naturally occurring isotopes, and the peaks to the left of the base peak (C_{10}BTA-4D and C_{10}BTA-5D) are due to 10% residual H_2O in the sample. One hour after the mixing, another aliquot was diluted into D_2O. Now, the mass spectrum clearly shows the presence of two different species of C_{10}BTA (Figure S6B). The base peak at m/z 626.4 corresponds to the double sodium adduct of C_{10}BTA-3D, and the peak at 627.9 corresponds to the double sodium adduct of C_{10}BTA-6D. Because the alcohols at the periphery of the monomers are in contact with water, C_{10}BTA-3D contains three deuterated alcohols and the amides have not been exchanged. Hence C_{10}BTA monomers enter the polymers formed from C_{12}BTA and causes C_{10}BTA-3D species to become more populated in the mass spectra when the mixture of the two BTAs is equilibrated for a longer time. At the same time, the contribution of the C_{10}BTA-6D species decreases (Figure S7). Hence, this new experimental approach for supramolecular polymers can be used to characterize the rates of copolymerization. Consistent with previous experiments, the presence of BTA-4D and BTA-5D in the mass spectra is fully due to the isotopes and residual H_2O in the sample.[S3]

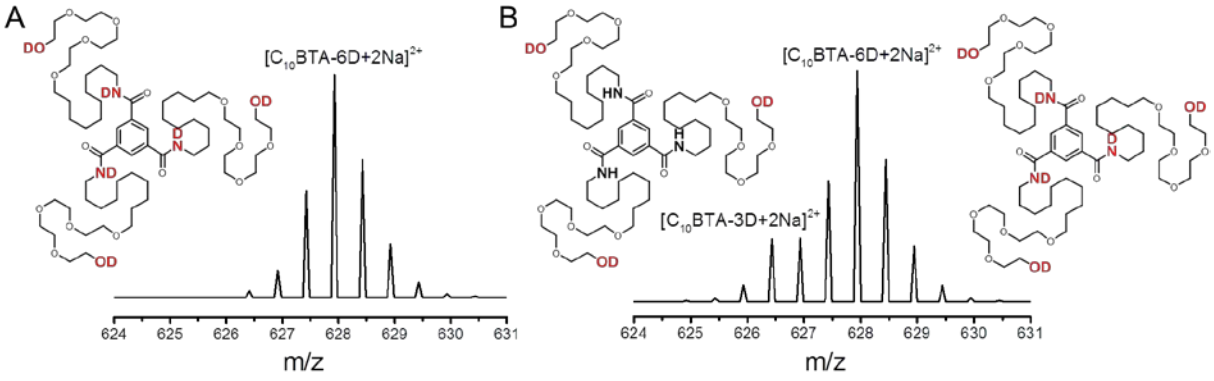

Figure S6. Mass spectra showing the doubly charged C_{10}BTA ions, acquired using 5 µM mixtures of C_{10}BTA and C_{12}BTA in D_2O/H_2O (9/1 v/v), and the chemical structures of C_{10}BTA-3D and C_{10}BTA-6D that correspond to the observed base peaks. The aggregates were mixed in H_2O for A) one minute, or B) 60 minutes.

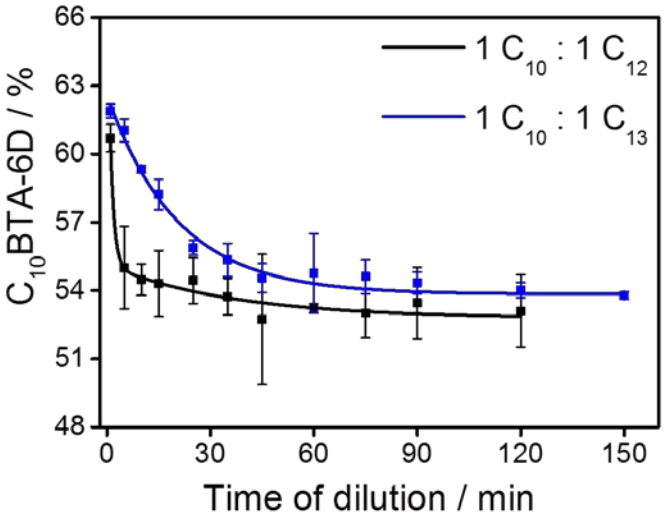

Figure S7. The percentage of C_{10}BTA-6D as a function of the mixing time (the time points at which aliquots were diluted into D_2O), when mixed at t = 0 minutes with polymers formed from C_{12}BTA (black) and C_{13}BTA (blue). The data points are an average of three separate measurements and the error bars represent one standard deviation of uncertainty. The solid lines are the following fitted exponential decay functions: C_{10}BTA-6D = 13.76*exp(-t/1.12) + 2.35*exp(-t/36.41) + 52.87 (R^2 = 0.99) (black) and C_{10}BTA-6D = 8.75*exp(-t/20.44) + 53.84 (R^2 = 0.99) (blue). The t_{50}'s that correspond to these fitted equations are ~2.3 minutes and ~15.2 minutes, respectively.

Influence of the experimental procedure and copolymer stability on the extent of HDX. The different maximum percentages of C_{10}BTA-3D that were attained by the mixtures cannot be interpreted in terms of molecular events; in addition to the molecular movements that occur during the 90 seconds exposure to D_2O, the copolymers that are being formed may have a different kinetic stability that is changing over time. To deepen our understanding of the kinetic differences observed for the variations in the alkyl chain length, we have also calculated and plotted the percentage of C_{12}BTA-3D and C_{13}BTA-3D of the corresponding copolymerization experiments with C_{10}BTA (Figure S8A). Curiously, we observed that during the first minutes the contribution of C_{12}BTA-3D is slightly increased, whereas for C_{13}BTA-3D a temporary decrease is observed. Hence, during the first minutes when C_{10}BTA already becomes incorporated in the polymers, C_{10}BTA also influences the amide HDX of the other component. This implies that there is a synergistic effect when C_{10}BTA is incorporated in the polymers formed from C_{12}BTA, because they were stabilized during the first minutes. Although these trends and the difference with C_{13}BTA are consistent with the first minutes of the kinetic traces displayed in Figure 4 of the main text, currently no experimental techniques are available to investigate these structures at both the time and spatial resolution required to provide further details. To exclude any influence of the mixing protocol on the HDX kinetics, we also mixed equimolar solutions containing the same BTA and plotted the percentage of BTA-3D as a function of the copolymerization time (Figure S8B). The absence of variations in BTA-3D% implies that the effects observed in Figure S8A are indeed due to the presence of C_{10}BTA.

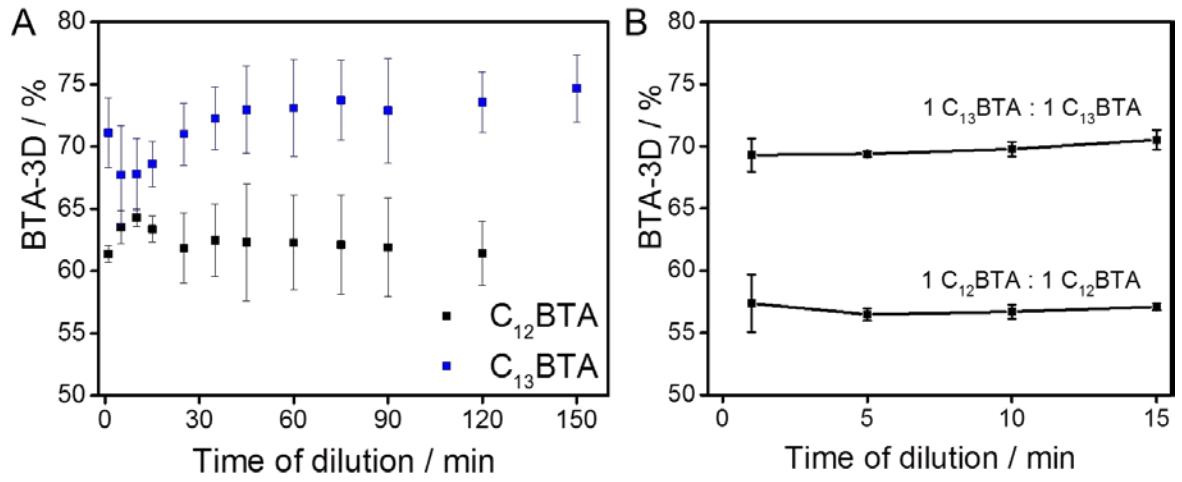

Figure S8. The percentage of C_{12}BTA-3D and C_{13}BTA-3D: A) as a function of the copolymerization time with C_{10}BTA and colored black and blue, respectively, and B) as a function of time after the 1:1 mixing with an equally concentrated BTA solution containing the same BTA. In both graphs, all data points are the average of three separate measurements and the error bars represent one standard deviation of uncertainty.

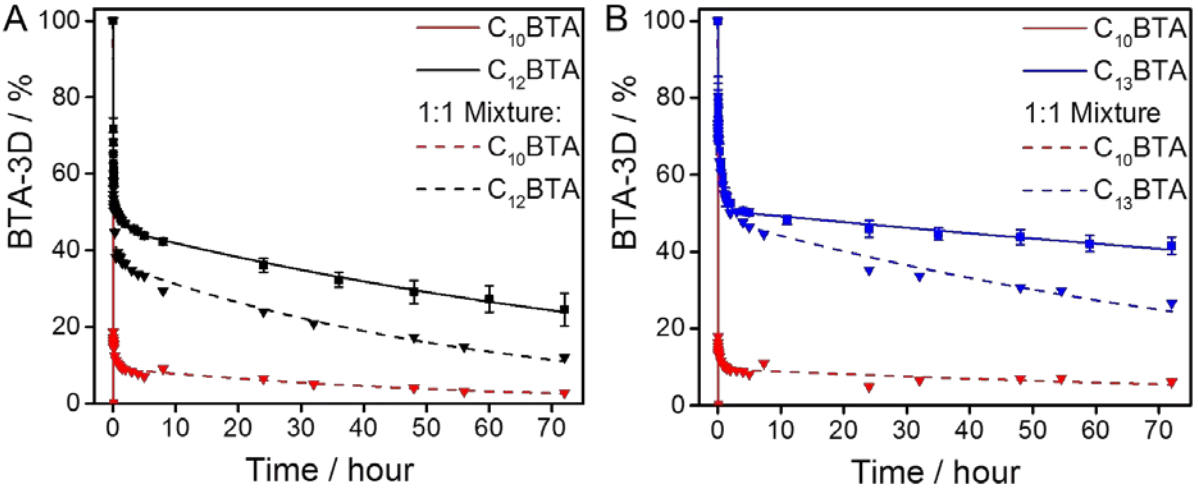

Figure S9. Solutions of the BTAs at 50 µM were mixed in a 1 : 1 molar ratio and equilibrated at room temperature overnight. The equilibrated copolymers were diluted once and 10-fold from H_2O into D_2O (t = 0 min). This sample in D_2O was subjected multiple times to ESI-MS. The solid lines were obtained from single-component solutions and were previously reported.[S4] The HDX of C_{10}BTA is slower in the mixtures with A) C_{12}BTA and B) C_{13}BTA (red, dashed lines), whereas the C_{12}BTA (black, dashed line) and C_{13}BTA (blue, dashed line) monomers in the mixtures exchange faster as compared to the single-component polymers. All lines are tri-exponential fits of the data that were obtained using our previously reported method.[S4]

MD simulations: model and methods. The CG models for C_{12}BTA and C_{13}BTA fibers, developed in the framework of the popular MARTINI force field,[S5] have been taken from a previous work.[S6] The C_{10}BTA monomer has been modelled by replacing the original C12 tails (composed by 4 SC1 MARTINI beads) with 1 C1 bead and 2 SC1 beads. Two cases were simulated, where the C_{10}BTA monomer would incorporate into a C_{12}BTA fiber (colored

black in all graphs) or into a C_{13}BTA fiber (blue in all graphs). A snapshot where the system is in state *(ii)* (see Figure S10) was generated for both fibers and 10 unbiased MD runs with different temperature seeds were conducted for 5 μs each. Then the incorporation of the new monomer into each fiber was monitored by measuring its coordination to the nearest hotspot with the analysis tools provided by PLUMED 2.3.2.[S7] A representative run and coordination measurement for each fiber is shown below in Figure S11. The GROMACS 5.1.2 and 2016.3 versions have been used for all simulations.[S8,S9] The parameters for all the unbiased MD simulations are reported in Supporting Table 1 below.

Supporting Table 1: Molecular Dynamics Simulation Parameters

Parameter	Value
Timestep	$0.02\ ps$
Periodic Boundaries	X, Y, Z
Thermostat	Velocity Rescale Params: • Temperature $= 300\ K$ • Time constant = $2.0\ ps$
Barostat	Semi-isotropic Berendsen Params: • Time constant $= 2.0\ ps$ • Compressibility $= 4.5 \times 10^{-5}\ \frac{1}{bar}$ • Pressure $= 1.0\ bar$
Constraints	None

The simulations revealed a large difference in incorporation time scales for the two fibers. The data from all simulation was analyzed to produce the Potential of Mean Force (PMF) shown in Figure S12. This suggested the existence of some difference in the free energy landscape of the incorporation process for the two fibers. Thus, well-tempered metadynamics simulations were carried out to investigate it.[S10] We did this with PLUMED 2.3.0,[S7] and GROMACS 2016.3 was patched with it. The collective variable used for these runs was the distance between the centers of mass of the C_{10}BTA monomer core and the center of mass of the nearest hotspot in the fiber. We used an upper wall to prevent the monomer from moving too far away from the hotspot and thus be able to achieve reasonable convergence. Four different profiles from each simulation have been averaged to obtain the free energy profile of Figure 6. Well-tempered metadynamics simulations parameters are reported in Table 2.

Supporting Table 2: Well-tempered metadynamics parameters used in PLUMED

Parameter	Value
Upperwall	AT = 1.2 EXP = 100.0 EPS=0.1
Well-tempered metadynamics	TEMP=300 BIASFACTOR = 20

	PACE=500 (= 10 ps) HEIGHT = 0.1 SIGMA=500 GRID_MIN=0 GRID_MAX=4 GRID_SPACING=0.001

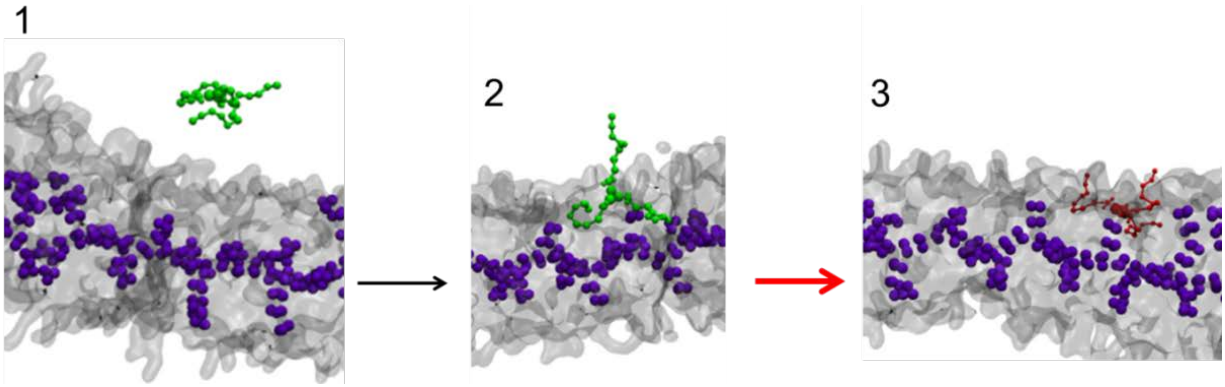

Figure S10. Steps of monomer incorporation: (1-2, *i-ii*) landing on the surface of the polymer and (2-3, *ii-iii*) incorporation into the hot-spot.

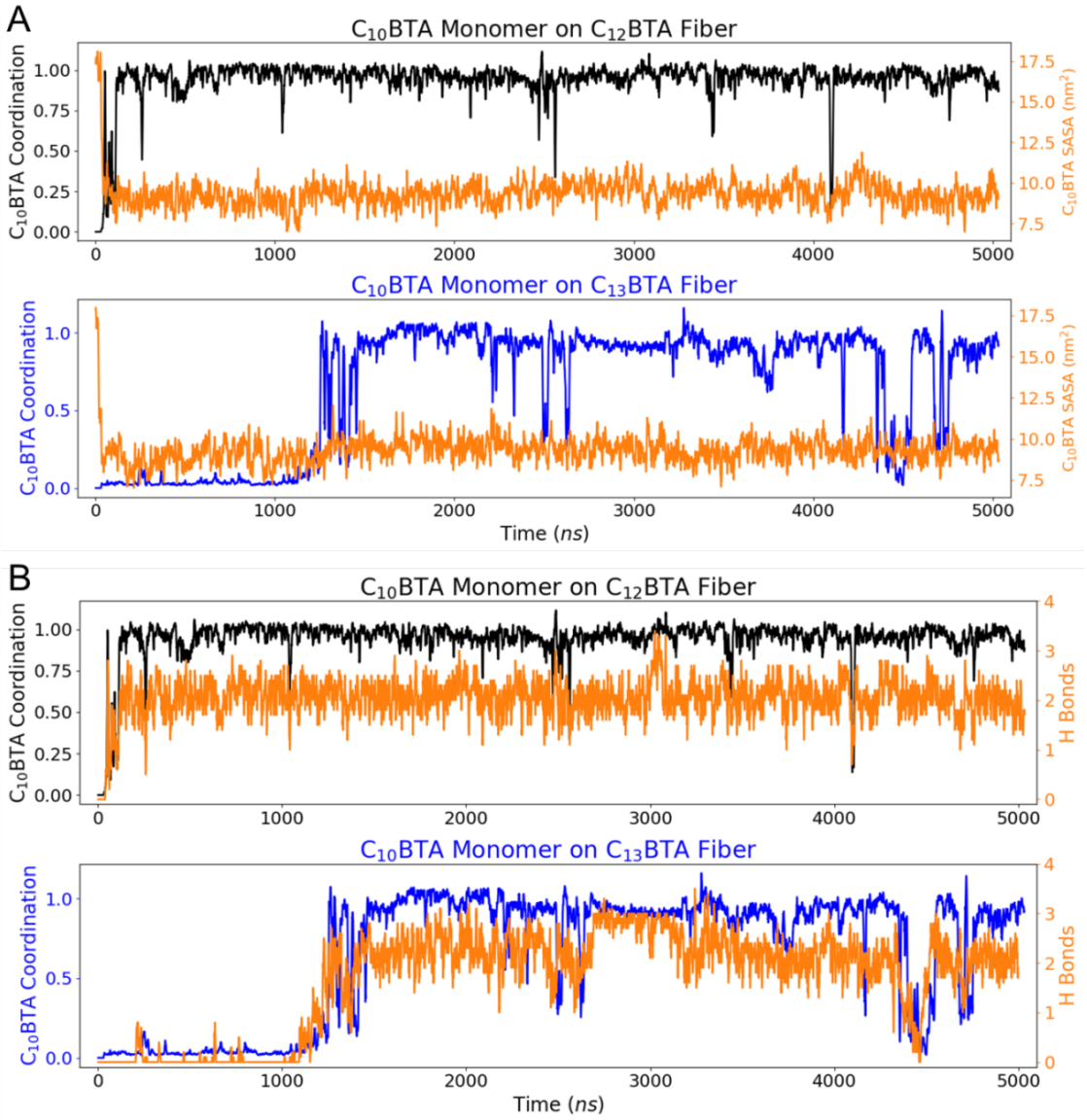

Figure S11. Correlations between core-core coordination and SASA (A, they are essentially independent) and between core-core coordination and the number of hydrogen bonds per-monomer (B, they are strongly correlated) in two example simulations.

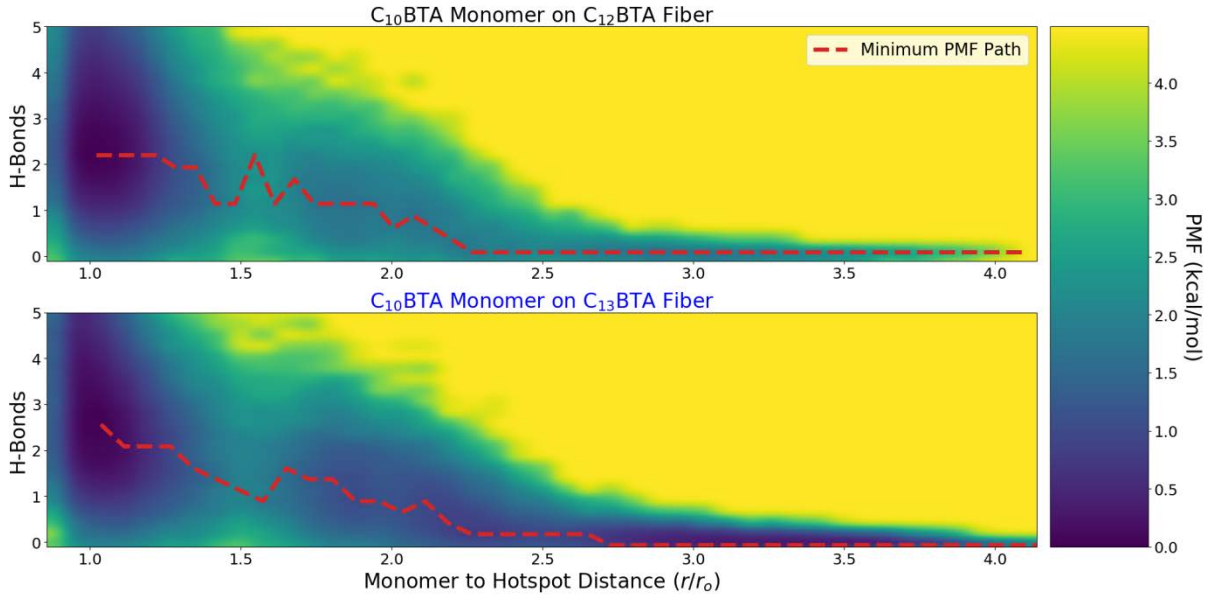

Figure S12. Free energy landscape obtained from merging all the unbiased CG-MD simulations data for C_{10}BTA monomer incorporation in a C_{12}BTA polymer (top) and in a C_{13}BTA polymer (bottom).

References

(S1) Leenders, C. M. A.; Baker, M. B.; Pijpers, I. A. B.; Lafleur, R. P. M.; Albertazzi, L.; Palmans, A. R. A.; Meijer, E. W., Supramolecular polymerisation in water; elucidating the role of hydrophobic and hydrogen-bond interactions. *Soft Matter* **2016,** *12* (11), 2887-2893.

(S2) Friedrich, H.; Frederik, P. M.; de With, G.; Sommerdijk, N. A. J. M., Imaging of Self-Assembled Structures: Interpretation of TEM and Cryo-TEM Images. *Angew. Chem., Int. Ed.* **2010,** *49* (43), 7850-7858.

(S3) Thota, B. N. S.; Lou, X.; Bochicchio, D.; Paffen, T. F. E.; Lafleur, R. P. M.; van Dongen, J. L. J.; Ehrmann, S.; Haag, R.; Pavan, G. M.; Palmans, A. R. A.; Meijer E. W., Supramolecular Copolymerization as a Strategy to Control the Stability of Self-Assembled Nanofibers. *Angew. Chem., Int. Ed.* **2018,** *57* (0), 6843-6847.

(S4) Lou, X.; Lafleur, R. P. M.; Leenders, C. M. A.; Schoenmakers, S. M. C.; Matsumoto, N. M.; Baker, M. B.; van Dongen, J. L. J.; Palmans, A. R. A.; Meijer, E. W., Dynamic diversity

of synthetic supramolecular polymers in water as revealed by hydrogen/deuterium exchange. *Nat. Commun.* **2017,** *8,* 15420.

(S5) Marrink, S. J.; Risselada, H. J.; Yefimov, S.; Tieleman, D. P.; de Vries, A. H., The MARTINI Force Field: Coarse Grained Model for Biomolecular Simulations. *J. Phys. Chem. B* **2007,** *111* (27), 7812-7824.

(S6) Bochicchio, D.; Pavan, G. M., From Cooperative Self-Assembly to Water-Soluble Supramolecular Polymers Using Coarse-Grained Simulations. *ACS Nano* **2017,** *11* (1), 1000-1011.

(S7) Tribello, G. A.; Bonomi, M.; Branduardi, D.; Camilloni, C.; Bussi, G., PLUMED 2: New feathers for an old bird. *Comput. Phys. Commun.* **2014,** *185* (2), 604-613.

(S8) Abraham, M. J.; Murtola, T.; Schulz, R.; Páll, S.; Smith, J. C.; Hess, B.; Lindahl, E., GROMACS: High performance molecular simulations through multi-level parallelism from laptops to supercomputers. *SoftwareX* **2015,** *1-2*, 19-25.

(S9) Hess, B.; Kutzner, C.; van der Spoel, D.; Lindahl, E., GROMACS 4: Algorithms for Highly Efficient, Load-Balanced, and Scalable Molecular Simulation. *J. Chem. Theory Comput.* **2008,** *4* (3), 435-47.

(S10) Barducci, A.; Bussi, G.; Parrinello, M., Well-Tempered Metadynamics: A Smoothly Converging and Tunable Free-Energy Method. *Phys. Rev. Lett.* **2008,** *100* (2), 020603.